ACS APPLIED BIO MATERIALS

www.acsabm.org Article

Enzyme-Free Colorimetric Immunoassay for Protein Biomarker Enabled by Loading and Disassembly Behaviors of Polydopamine Nanoparticles

Li Li, Zhenyuan Xing, Qiaorong Tang, Lei Yang, Li Dai, Huan Wang, Tao Yan, Weiying Xu, Hongmin Ma,* and Qin Wei

Cite This: https://dx.doi.org/10.1021/acsabm.0c01167 Read Online

ACCESS | Metrics & More | Article Recommendations | Supporting Information

ABSTRACT: In this work, a mussel-inspired polydopamine (PDA) nanoparticle with biocompatible and reactive surface characteristics was desirably incorporated with high loading capacity and pH-induced disassembly-releasing behavior toward Fe(III) ions to develop an enzyme-free colorimetric immunoassay. The catechol functional network of PDA can act as a scaffold to coordinate with large amounts of Fe(III) ions to form the PDA-Fe(III) NPs whose coordination state can be tailored by changing the pH values. In detail, PDA-Fe(III) NPs can be maintained in a disassembled tri-coordinate state under alkaline conditions while the highly loaded Fe(III) ions can be easily released under acid conditions to react with ferrocyanide for the in situ generation of Prussian blue (PB) NPs. The detection sensitivity of prostate-specific antigen (PSA) was significantly improved, owing to the high peroxidase-like activity of PB NPs that triggered excellent catalytic effect by the colorimetric reaction. In addition, favorable linearity was found in the range of 0.0005−20 ng mL^{-1} with a low detection limit of 0.84 pg mL^{-1} (S/N = 3). Furthermore, excellent selectivity and reproducibility were exhibited by the developed enzyme-free colorimetric immunoassay. It is believed that this proposed PDA-Fe(III) NP-based enzyme-free colorimetric system will offer a facile and reliable tool for the sensitive detection of PSA and other cancer biomarkers in human serum.

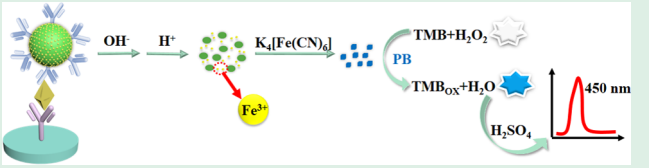

KEYWORDS: *cancer biomarker, Prussian blue, nanozyme, biosensor, ELISA, melanin-like nanoparticles*

INTRODUCTION

The enzyme-linked immunosorbent assay (ELISA) is the most widely used immunoassay for biomarker detection, which is also regarded as a standard method to evaluate the feasibility and reliability of the newly developed immunoassays. Although optical-based biosensors with reproducible sensing surfaces have been widely used in medicine and other fields, ELISA shows more fascinating merits such as ease of operation, automated high throughput, and excellent sensitivity.[1−3] In recent years, significant achievements for this technique have been fulfilled by employing some advanced nanomaterials as sensing elements,[4−6] among which the use of nanomaterials to label both detection antibody and signaling enzyme brings lots of interest.[7] Nanomaterials with a large surface area are able to attach a large number of enzymes and antibodies to promote the detection sensitivity through signal amplification.[8,9] In particular, various catalytic nanomaterials as signal tags for detection antibody[10] show more favorable stability and accessibility than natural enzymes, thus showing great potential for being enzyme alternatives in developing enzyme-free colorimetric immunoassays.[11,12]

Prussian blue (PB) is well known for the excellent peroxidase-like activity toward the reduction of H_2O_2.[13] However, the application of PB nanoparticles (PB NPs) as signal labels in sandwich-type colorimetric immunoassays is limited.[14,15] On the one hand, the capping ligands used to control the nanostructure morphology usually decrease the catalytic activity. On the other hand, due to the coordination nature of PB, it finds it difficult to form bioconjugates with the detection antibody. Considering the easy formation protocol by mixing solutions of mixed-valence hexacyanide, an elegant strategy was proposed of using iron-containing nanomaterials as PB precursors.[16,17] The in situ derived iron ions were used to form PB and generate colorimetric signals. The application of these iron-containing nanomaterials still needs complex surface functionalization and the release of iron ions is achieved under harsh conditions. It is very desirable to construct loading and release systems for iron ions that are compatible with the colorimetric immunoassays.

Mussel-inspired polydopamine (PDA) coating, a universal surface engineering method for solid substrates and nano-

Received: September 14, 2020
Accepted: November 28, 2020

Scheme 1. (A) Preparation Process of PDA-Fe(III) NPs and PDA-Fe(III)-Ab_2. (B) Fabrication Process of the Colorimetric Immunosensor. (C) Sensing Mechanism for the PB-Induced Colorimetric Immunoassay

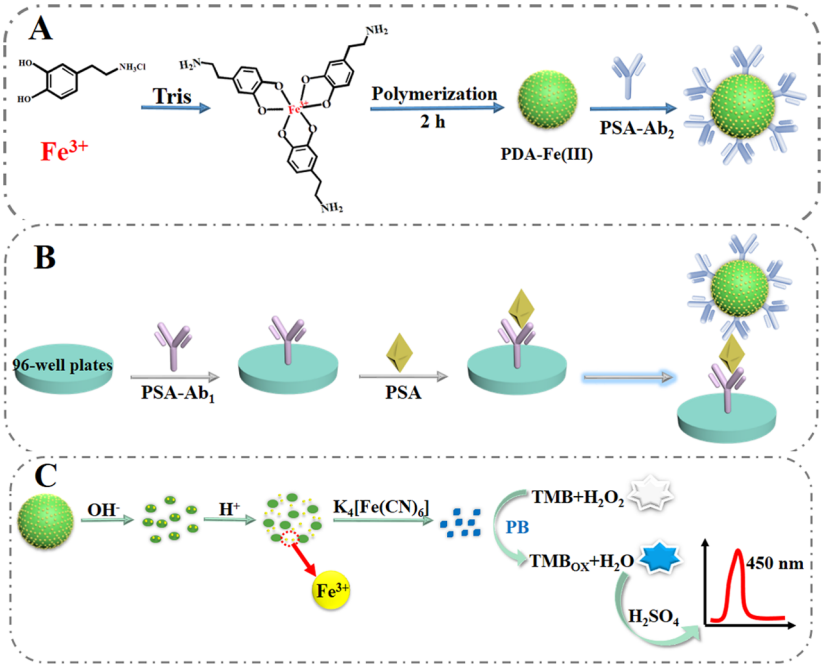

particles,[18] owns a superadhesive property that can improve the biocompatibility for surface modification of materials.[19−21] The biocompatible and active PDA layers enable the facile immobilization of biomolecules and have found good application in constructing various sensing interfaces.[22] The auto-oxidation of dopamine in basic conditions produces melanin-like nanoparticles that have surface properties similar to those of PDA thin films.[23] In the previous works, we have shown the easy fabrication of different immunosensors using PDA NPs as labels based on the surface reactive properties.[24,25] The abundant catechol groups present in PDA NPs show unique chelating affinity to transition metal ions.[26] The PDA NPs with a high loading capacity of paramagnetic metal ions have aroused considerable interest in biomedical fields,[27,28] including magnetic resonance imaging and cancer therapy.[29] The chelating interaction between catechol groups and Fe(III) ions is pH-dependent and has been used in the pH-responsive film disassembly.[30] It has been demonstrated that PDA NPs also show an alkaline-induced dissociated behavior,[31,32] further indicating the great potential of using PDA NPs to device a loading and release system for Fe(III) ions.

Inspired by that, a highly effective PB-based colorimetric immunoassay using PDA-Fe(III) NPs as signal labels was inspiringly developed for biomarker detection. Notably, the high loading capacity of Fe(III) ions was achieved on PDA-Fe(III) NPs by chelating interaction. By virtue of the pH-induced disassembly of PDA, Fe(III) ions can be rapidly released in the solution to generate PB NPs in situ without capping ligands. Based on the high peroxidase-like activity of PB NPs, an excellent catalytic effect was triggered during the colorimetric reaction, which significantly improved the detection sensitivity when using prostate-specific antigen (PSA) as the target analyte. It is believed that this proposed PDA-Fe(III) NP-based enzyme-free colorimetric system will offer a facile and reliable tool for the sensitive detection of PSA and other cancer biomarkers in human serum.

MATERIALS AND METHODS

Reagents and Apparatus. Tris(hydroxymethyl)aminomethane (Tris) was obtained from Macklin (Shanghai, China). 3,3′,5,5′-Tetramethylbenzidine (TMB) was purchased from Tokyo Chemical Industry Co. Ltd. Bovine serum albumin (BSA, 96−99%) was obtained from Aladdin Ltd. (Shanghai, China). PSA and its capture antibody (Ab_1) and detection antibody (Ab_2) were bought from Shanghai Linc-Bio Science Co. Ltd. (Shanghai, China). The other details were provided in the Supporting Information.

Preparation of PDA-Fe(III) NPs. The preparation of PDA-Fe(III) NPs was performed according to the previously reported prepolymerization doping strategy with some slight modifications.[33] The synthesis process of PDA-Fe(III) NPs is described in Scheme 1A: First, 45 mg of dopamine and 6.2 mg of $FeCl_3{\cdot}6H_2O$ were fully dissolved in 130 mL of deionized water for 1 h under stirring at room temperature. Next, 20 mL of Tris solution (22.5 mg mL^{-1}) was added to the mixture solution and stirred for 2 h. Then, the resulting product was washed with ultrapure water five times and redispersed in 10 mL of deionized water.

Preparation of PDA-Fe(III)-Ab_2. The preparation process of PDA-Fe(III)-Ab_2 bioconjugate is depicted in Scheme 1A. First, 1 mL of the detection antibody (Ab_2, 1 μg mL^{-1}) was mixed with 1 mL of PDA-Fe(III) NPs dispersion and incubated at 4 °C for 6 h. Since PDA-Fe(III) NPs have catechol groups on the surface, they can be combined with amine-terminated Ab_2 via the Michael addition or Schiff base reaction.[34] Then, the above solution was mixed with 100 μL of BSA (1%), which could close the nonspecific sites, followed by centrifuging and washing with ultrapure water to remove unbound bioconjugate and BSA. Finally, the PDA-Fe(III)-Ab_2 bioconjugate was redispersed in 1 mL of phosphate-buffered saline (PBS, pH 7.4) for further use.

Procedure of the Colorimetric Immunoassay. The detailed fabrication process of the colorimetric immunosensor is demonstrated in Scheme 1B. After each step below, the modified 96-microwell plate was washed with PBS solution three times to eliminate the unabsorbed species. First, 100 μL of Ab_1 (1 μg mL^{-1}) was incubated on the plate for 12 h at 4 °C. Due to the hydrophobic interaction, Ab_1

https://dx.doi.org/10.1021/acsabm.0c01167
ACS Appl. Bio Mater. XXXX, XXX, XXX−XXX

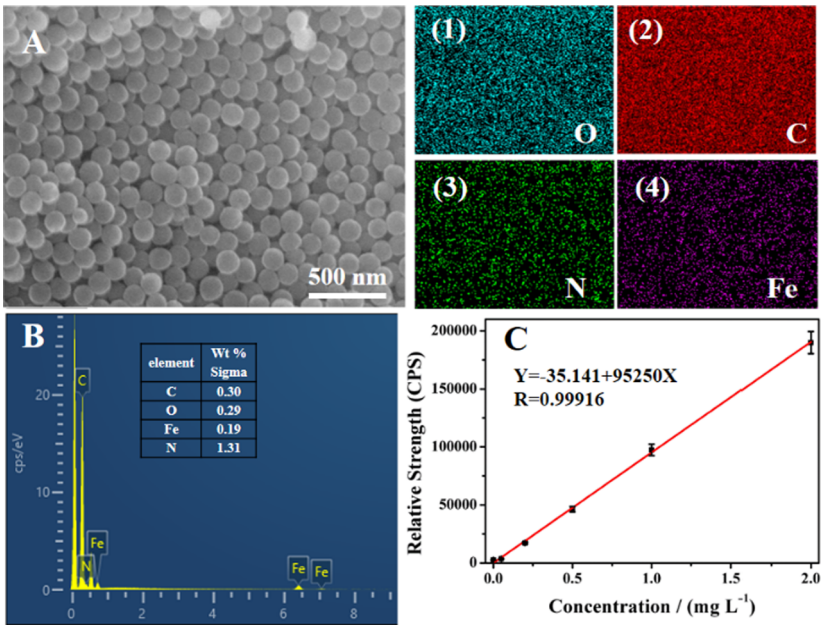

Figure 1. SEM and element mapping images of O (1), C (2), N (3), and Fe (4) in PDA-Fe(III) NPs (A). EDS spectrum of PDA-Fe(III) NPs (B). Calibration curve measured by ICP-OES (C).

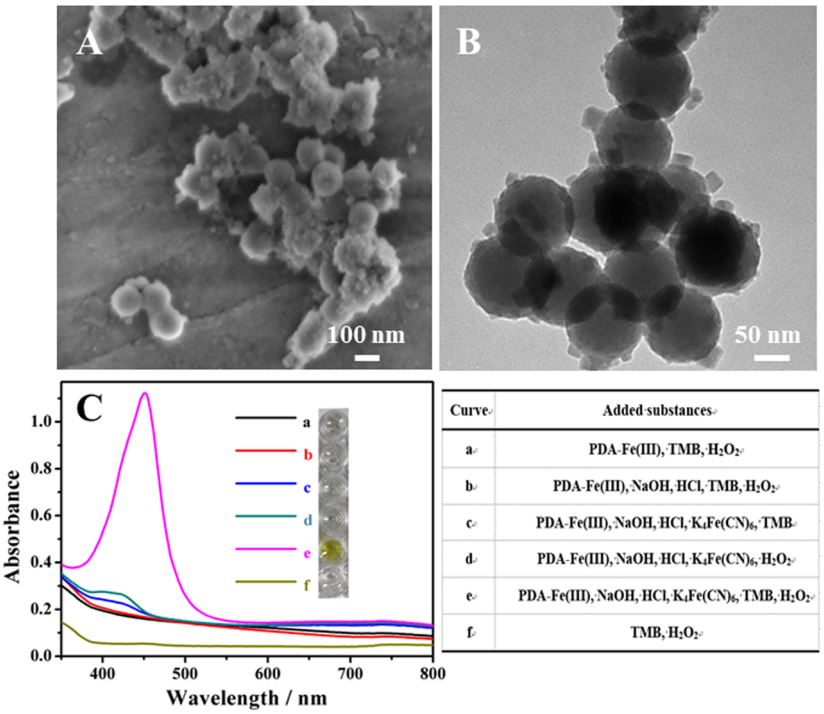

Figure 2. SEM images (A) and TEM images (B) of the PB generated based on PDA-Fe(III) NPs. UV−vis spectrum (C) of the test solution (inset table shows the added substances included in the test solution).

can be physically adsorbed on the surface of a 96-well microplate made of polystyrene.[35,36] Then, the nonspecific activity sites were blocked with 1% BSA (100 μL) and incubated at room temperature for 1 h. Afterward, 100 μL of different concentrations of PSA were added into the wells and incubated for 1 h at 37 °C. Following that, 100 μL of the PDA-Fe(III)-Ab_2 bioconjugate was incubated on the well for sandwiched immunoreaction for 1 h at room temperature. Noteworthily, Ab_1 and Ab_2 were different antibodies. Ab_1 was a capture antibody that captured the test antigen, while Ab_2 was a detection antibody that could bind to the captured antigen.[37] Both Ab_1 and Ab_2 had high specificity for antigens, and there was no competitive binding between them and antigens because they bind antigens at different sites. Next, as shown in Scheme 1C, Fe(III) ions derived in situ from Fe(III) ion-loaded PDA NPs were used to form PB and generated colorimetric signals. After cleaning the wells three times with ultrapure water, 1 mol L^{-1} NaOH solution (28 μL) was added to each well to dissociate the iron-loaded dopamine shell. Then, the pH environment was adjusted with 30 μL of 1 mol L^{-1} HCl solution to release Fe^{3+} into the solution. Afterward, 30 μL of 2 mmol L^{-1} $K_4Fe(CN)_6$ solution was added to each well and PB was formed through the complexation reaction. Following that, TMB (100 μL) and H_2O_2 (100 μL) reagents were added to the well to produce a

https://dx.doi.org/10.1021/acsabm.0c01167
ACS Appl. Bio Mater. XXXX, XXX, XXX−XXX

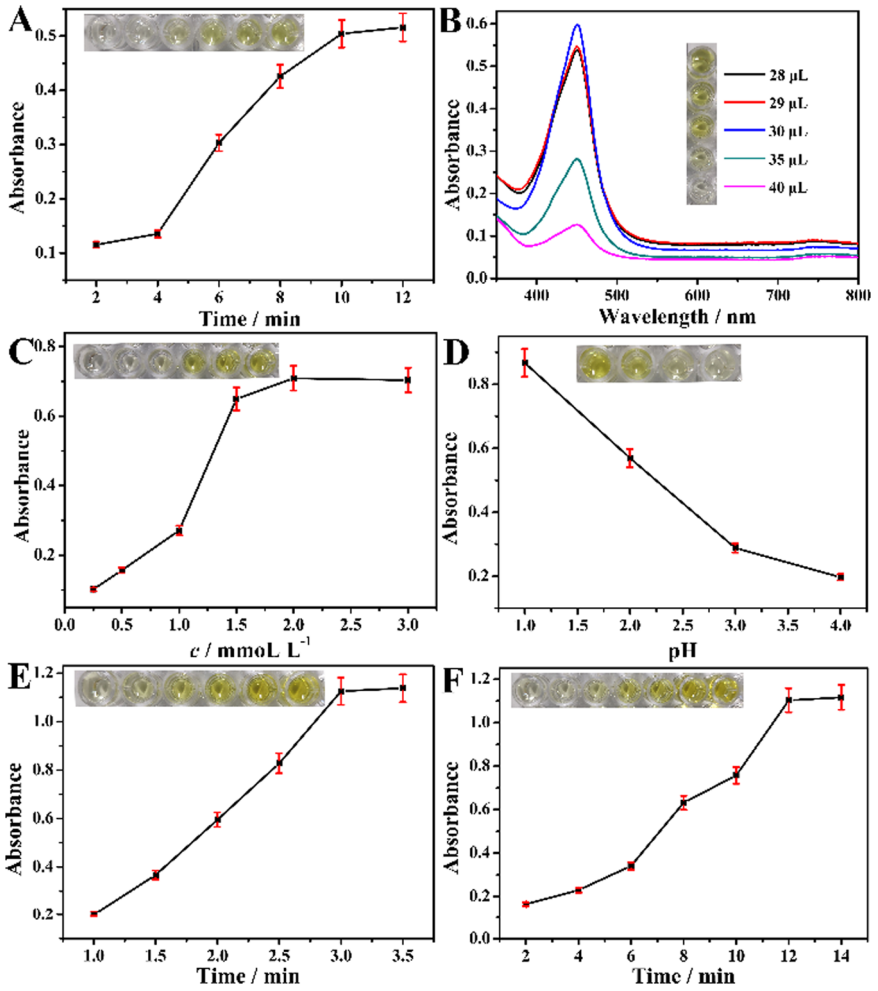

Figure 3. Effects of the decomposition time of iron-loaded dopamine shell in the NaOH solution (A), volume of the HCl solution (B), concentration of the $K_4Fe(CN)_6$ solution (C), pH of the $K_4Fe(CN)_6$ solution (D), complexation reaction time of the $K_4Fe(CN)_6$ and Fe^{3+} solution (E), and reaction times of TMB and H_2O_2 (F) for the detection 1 ng mL^{-1} PSA.

color reaction. Finally, 1 mol L^{-1} H_2SO_4 solution (50 μL) was dropped into each well to stop the color reaction and render the solution yellow. The absorbance intensities were detected at a wavelength of 450 nm.

The process of horseradish peroxidase (HRP)-ELISA was the same as the PDA-Fe(III) NPs-ELISA apart from the substitutions of PDA-Fe(III)-Ab_2 conjugates with 1 μg mL^{-1} of HRP-Ab_2 conjugates (100 μL). Next, TMB (100 μL) and H_2O_2 (100 μL) reagents were added to the well and incubated at room temperature for 12 min. Finally, 50 μL of 1 mol L^{-1} H_2SO_4 solution was dropped into the wells and the absorbance value was also detected at a wavelength of 450 nm.

RESULTS AND DISCUSSION

Characterization of the PDA-Fe(III) NPs. Compositional and morphological data of the as-synthesized PDA-Fe(III) NPs were characterized. As seen in Figure 1A, the scanning electron microscopy (SEM) image of PDA-Fe(III) NPs showed the characteristics of a spherical surface with a uniform surface, with a diameter of about 150 nm, and the corresponding element mapping analysis (1−4) also confirmed the uniform distribution of N, C, O, and Fe elements. Energy-dispersive spectrometry (EDS) was conducted to show the element composition of nanomaterials. As shown in Figure 1B, PDA-Fe(III) NPs were confirmed to contain Fe, C, O, and N elements. In addition, the surface charge of the nanomaterials was revealed by the ζ-potential in Figure S1. The surface charge of PDA NPs was −49.6 mV (a), which was due to the functional catechol group. With the addition of positively charged Fe (III) ions, the surface charge of PDA-Fe(III) NPs became −37.0 mV (b), indicating that Fe(III) ions were successfully loaded by PDA NPs. The above results indicated that the preparation of PDA-Fe(III) NPs was successful.

The Fe(III) ion content of PDA-Fe(III) NPs was detected by inductively coupled plasma-optical emission spectrometry (ICP-OES). The calibration curve of elemental iron is shown in Figure 1C. Detailed test data is listed in Table S1. It was calculated that the iron content in PDA-Fe(III) NPs was about 7.76 μg mg^{-1}. Abundant iron ions could efficiently generate PB NPs in situ, which triggered excellent catalysis in the colorimetric reaction.

Formation of Catalytic PB from Fe(III)-Loaded PDA. The possibility of PDA-Fe(III) NPs generating PB is illustrated in Figure 2. As shown in the SEM (Figure 2A) and transmission electron microscopy (TEM) (Figure 2B) images, the PB cubes were dispersed on the surface of PDA-Fe(III) NPs after alkali decomposition for 1 min. These results indicated that PDA-Fe(III) NPs can successfully form PB through pH adjustment.

The importance of the HCl solution in the reaction is investigated in Figure S2 (inset I was the addition of $K_4Fe(CN)_6$ solution, II was H_2SO_4 solution to stop the

https://dx.doi.org/10.1021/acsabm.0c01167
ACS Appl. Bio Mater. XXXX, XXX, XXX−XXX

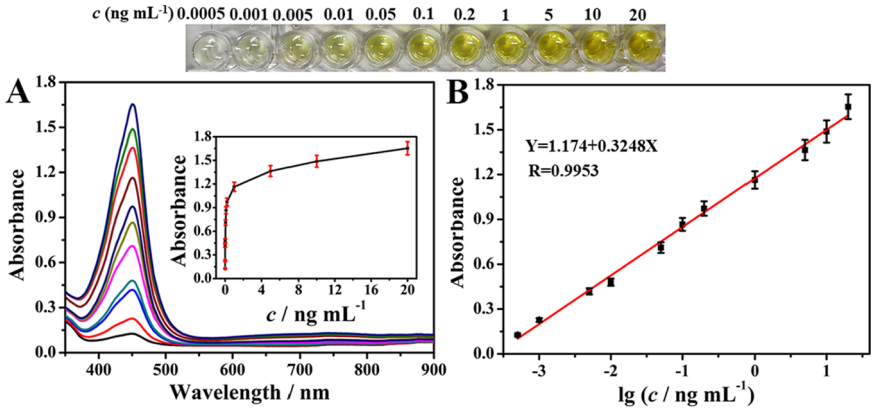

Figure 4. UV−vis spectra of the proposed immunosensor based on PDA-Fe(III) NPs (A) for different concentrations of PSA from 0.0005 to 20 ng mL^{-1} (the inset was the calibration curve between the absorbance and PSA). Calibration curve based on the absorbance toward the logarithmic value of PSA (B). Error bar = relative standard deviation (RSD) (n = 3).

reaction). During the process of adding HCl solution (1), the color of the solution changed from blue forming PB to yellow with an absorption peak at 450 nm (curve a). In contrast, in the process without adding the HCl solution (2), the solution was always light gray and no absorption peak appeared at 450 nm (curve b). The above two comparisons showed that the acidic environment after the addition of the HCl solution would effectively reduce the coordination number of the catechol groups, thereby allowing Fe^{3+} to be released in the solution and generated PB. Therefore, adjusting the pH of the solution with HCl was critical for the successful production of PB.

Characterization of Peroxidase-Like Activity of Nanomaterials. To confirm the peroxidase-like activity of nanomaterials, a typical chromogenic reaction was studied by the catalytic oxidation of TMB with the help of H_2O_2. As shown in Figure 2C, the simple mixed solution of TMB and H_2O_2 was colorless and did not show an absorption peak in the wavelength range of 350−800 nm (curve f). Also, the catalysis of PDA-Fe(III) NPs did not show an absorption peak (curve a), indicating that it had no peroxidase properties. Then, PDA-Fe(III) NPs dispersion was added with NaOH and HCl solution to release Fe^{3+} to catalyze the oxidation of TMB in the presence of H_2O_2.

As a result, no absorption peak appeared (curve b), indicating that Fe^{3+} did not have peroxidase properties. As shown in Figure S3, the pure $K_4Fe(CN)_6$ solution catalyzed oxidation of TMB by H_2O_2 was colorless and showed no absorption peak in the wavelength range of 350−800 nm (curve a). Immediately after the addition of H_2SO_4, there was no absorption peak at 450 nm (curve b), indicating that $K_4Fe(CN)_6$ cannot catalyze the oxidation of TMB by H_2O_2. Besides, there was also no absorption peak with the addition of only TMB (curve c) or H_2O_2 (curve d) into the solution in which PB was formed from PDA-Fe(III) NPs, while the addition of TMB and H_2O_2 at the same time would produce an absorption peak at 450 nm (curve e). Hence, the presence of H_2O_2 was a precondition for the development of visible color. The above studies indicate that in situ generated PB NPs by the reaction between the released Fe(III) ions and ferrocyanide has excellent peroxidase-like activity.

Optimization of the Detection Condition. To achieve the best performance of the prepared colorimetric immunoassay, experimental conditions were optimized in this work. In the beginning, the decomposition time of the iron-loaded dopamine shells in the NaOH solution was investigated. As presented in Figure 3A, the absorbance increased with increasing decomposition time and reached a maximum at 10 min. Therefore, 10 min was considered to be the best time to decompose the iron-loaded dopamine shell in the NaOH solution. The effect of different volumes of HCl solution on the release of Fe^{3+} is shown in Figure 3B. It was found that the maximum absorbance intensity presented when the volume of the HCl solution was 30 μL, which may be due to the fact that more or less HCl solution would affect the release of Fe^{3+} and the formation of PB. The concentration of the $K_4Fe(CN)_6$ solution played a crucial role in the complexation reaction to produce PB. As seen in Figure 3C, the absorption intensity increased with the increase in the $K_4Fe(CN)_6$ solution concentration and reached a maximum at 2 mmol L^{-1}. Therefore, a 2 mmol L^{-1} $K_4Fe(CN)_6$ solution was selected as the optimum concentration for the entire experiment.

In addition, the pH of the $K_4Fe(CN)_6$ solution was of great significance for the formation and catalytic effect of PB. As shown in Figure 3D, the absorbance intensity reached a maximum under strong acidic conditions of pH = 1. Also, the pH after adding TMB and H_2O_2 solutions was about 4.3, which was consistent with the reported optimal pH results of the oxidation of TMB by H_2O_2.[38] Thus, pH = 1 was regarded as the optimal pH value of the $K_4Fe(CN)_6$ solution. Next, Figure 3E depicts the signal response of the reaction time of Fe^{3+} and $K_4Fe(CN)_6$ to absorbance. When the reaction time was 3 min, the absorbance reached a maximum because $K_4Fe(CN)_6$ and Fe^{3+} were completely reacted at this time. Figure 3F shows that the absorbance increased with increasing TMB and H_2O_2 reaction times and reached a maximum at 12 min. Thus, the optimum catalytic oxidation reaction time for the activity of nanozymes was set at 12 min.

Analytical Performance of the Colorimetric Immunoassay. Under optimal conditions, the colorimetric immunosensors with the secondary antibody markers were tested with a PSA linear detection range of 0.0005−20 ng mL^{-1}. Figure 4A depicts that the absorbance density at 450 nm increased with the increasing PSA concentration in the sample. The linear calibration curve of PDA-Fe(III) NPs as the marker was $y = 1.174 + 0.3248 \lg c$ (R = 0.9953) in Figure 4B, and the detection limit was 0.84 pg mL^{-1} (S/N = 3). In comparison, the detection limit of HRP-ELISA was calculated to be 6.81 pg

https://dx.doi.org/10.1021/acsabm.0c01167
ACS Appl. Bio Mater. XXXX, XXX, XXX−XXX

mL^{-1} according to its calibration curve (b, Figure S4), which was much higher than that of PDA-Fe(III) NPs-ELISA. Compared to the previously reported work (Table S2), the proposed colorimetric immunosensors showed a lower detection limit and a wider linear range, which could be attributed to the excellent catalytic effect of PB NPs generated by PDA-Fe(III) NPs with a high loading of Fe(III) ions.

Selectivity and Reproducibility of the Colorimetric Immunoassay. Owing to the presence of nonspecific adsorption, it is critical that the sensing system exhibits a good specificity for the target analyte.[39,40] Thus, the selectivity of the proposed colorimetric immunosensor for PSA was investigated. Several potential interfering compounds including carcinoembryonic antigen (CEA), α-fetoprotein (AFP), and BSA with a concentration of 100 ng mL^{-1} were chosen to testify to the selectivity of the immunosensor. As shown in Figure S3A, there were no remarkable differences among the absorbance intensities detected from the mixed samples and the PSA sample (10 ng mL^{-1}). Only the PSA sample and the mixed sample showed a significant color change at 450 nm, while other interfering proteins had a negligible color response, indicating a satisfactory specificity.

The reproducibility of colorimetric immunosensor was assessed using the same conditions. As proved in Figure S3B, six groups of immunoassays for 10 ng mL^{-1} PSA were carried out, respectively. It was confirmed that the prepared colorimetric immunosensor had a favorable reproducibility and the RSD was 2.26%.

Analysis in Real Samples. A standard addition method was used to test the concentration of PSA in serum samples (Table 1) so as to evaluate the feasibility and accuracy of the colorimetric immunoassay in practical analysis. Standard PSA serum samples of different concentrations of 0.10, 1.00, and 5.00 ng mL^{-1} were pipetted into the serum samples. The average recovery of the immunosensor was between 100.6 and 102.0% with an RSD of 0.73−3.61% (<5%). The results revealed that the proposed immunosensor could be safely utilized for the detection of PSA in the serum samples.

Table 1. Results of the PSA Determination in Serum Sample

serum PSA (ng mL^{-1})	added (ng mL^{-1})	detection content (ng mL^{-1}, n = 5)	mean (ng mL^{-1})	RSD (%)
0.43	0.10	0.54, 0.56, 0.52, 0.51, 0.53	0.53	3.61
	1.00	1.44, 1.49, 1.43, 1.41, 1.47	1.45	2.21
	5.00	5.44, 5.46, 5.41, 5.49, 5.51	5.46	0.73

CONCLUSIONS

In this work, PDA-Fe(III) composites, synthesized by the prepolymerization doping strategy, were used to label the detection antibody of a cancer biomarker PSA for constructing an efficient PB-based enzyme-free colorimetric immunoassay. Benefiting from the high loading capacity of Fe(III) ions and the pH-induced disassembly-releasing behaviors of PDA layers, PB NPs were effectively in situ generated to catalyze the colorimetric reaction, thus achieving a higher sensitivity during the detection. Using the developed biosensor to monitor the concentration of PSA in human serum, excellent linearity between 0.5 pg mL^{-1} and 20 ng mL^{-1} with a low detection limit of 0.84 pg mL^{-1} was achieved along with favorable specificity and reproducibility. Considering the above advantages, this proposed colorimetric immunoassay based on a biocompatible PDA-Fe(III)-based catalytic system holds great potential for the sensitive detection of cancer biomarkers.

ASSOCIATED CONTENT

Supporting Information

The Supporting Information is available free of charge at https://pubs.acs.org/doi/10.1021/acsabm.0c01167.

Materials and reagents, apparatus, ζ-potential characterization, determination of Fe(III) ions content, Fe(III) ion content of PDA-Fe(III) NPs (Table S1), UV−vis absorbance spectrum, and the developed colorimetric biosensors for detecting PSA compared to other published common existing biosensor (Table S2) (PDF)

AUTHOR INFORMATION

Corresponding Author

Hongmin Ma − *Collaborative Innovation Center for Green Chemical Manufacturing and Accurate Detection, Key Laboratory of Interfacial Reaction & Sensing Analysis in Universities of Shandong, School of Chemistry and Chemical Engineering, University of Jinan, Jinan 250022, P. R. China;* orcid.org/0000-0002-7061-8944; Email: mahongmin2002@126.com

Authors

Li Li − *Collaborative Innovation Center for Green Chemical Manufacturing and Accurate Detection, Key Laboratory of Interfacial Reaction & Sensing Analysis in Universities of Shandong, School of Chemistry and Chemical Engineering, University of Jinan, Jinan 250022, P. R. China*

Zhenyuan Xing − *Collaborative Innovation Center for Green Chemical Manufacturing and Accurate Detection, Key Laboratory of Interfacial Reaction & Sensing Analysis in Universities of Shandong, School of Chemistry and Chemical Engineering, University of Jinan, Jinan 250022, P. R. China*

Qiaorong Tang − *Collaborative Innovation Center for Green Chemical Manufacturing and Accurate Detection, Key Laboratory of Interfacial Reaction & Sensing Analysis in Universities of Shandong, School of Chemistry and Chemical Engineering, University of Jinan, Jinan 250022, P. R. China*

Lei Yang − *Collaborative Innovation Center for Green Chemical Manufacturing and Accurate Detection, Key Laboratory of Interfacial Reaction & Sensing Analysis in Universities of Shandong, School of Chemistry and Chemical Engineering, University of Jinan, Jinan 250022, P. R. China*

Li Dai − *Collaborative Innovation Center for Green Chemical Manufacturing and Accurate Detection, Key Laboratory of Interfacial Reaction & Sensing Analysis in Universities of Shandong, School of Chemistry and Chemical Engineering, University of Jinan, Jinan 250022, P. R. China*

Huan Wang − *Collaborative Innovation Center for Green Chemical Manufacturing and Accurate Detection, Key Laboratory of Interfacial Reaction & Sensing Analysis in Universities of Shandong, School of Chemistry and Chemical Engineering, University of Jinan, Jinan 250022, P. R. China*

Tao Yan − *Collaborative Innovation Center for Green Chemical Manufacturing and Accurate Detection, Key Laboratory of Interfacial Reaction & Sensing Analysis in Universities of Shandong, School of Chemistry and Chemical*

Engineering, University of Jinan, Jinan 250022, P. R. China; orcid.org/0000-0002-8073-691X

Weiying Xu − *Collaborative Innovation Center for Green Chemical Manufacturing and Accurate Detection, Key Laboratory of Interfacial Reaction & Sensing Analysis in Universities of Shandong, School of Chemistry and Chemical Engineering, University of Jinan, Jinan 250022, P. R. China*

Qin Wei − *Collaborative Innovation Center for Green Chemical Manufacturing and Accurate Detection, Key Laboratory of Interfacial Reaction & Sensing Analysis in Universities of Shandong, School of Chemistry and Chemical Engineering, University of Jinan, Jinan 250022, P. R. China;* orcid.org/0000-0002-3034-8046

Complete contact information is available at: https://pubs.acs.org/10.1021/acsabm.0c01167

Notes

The authors declare no competing financial interest.

■ ACKNOWLEDGMENTS

This study was financially supported by the National Natural Science Foundation of China (21675063), A Project of Shandong Province Higher Educational Youth Innovation Science and Technology Program (2020KJC008), and the Jinan Scientific Research Leader Workshop Project (2018GXRC021 and 2018GXRC024).

■ REFERENCES

(1) Wang, R.; Zhu, X.; Xing, Y.; Memon, A. G.; Shi, H.; Zhou, X. Multitag-regulated cascade reaction: A generalizable ultrasensitive microRNA biosensing approach for cancer prognosis. *ACS Appl. Mater. Interfaces* **2019**, *11*, 36444−36448.

(2) Liu, L.; Zhou, X.; Lu, Y.; Shan, D.; Xu, B.; He, M.; Shi, H.; Qian, Y. Facile screening of potential xenoestrogens by an estrogen receptor-based reusable optical biosensor. *Biosens. Bioelectron.* **2017**, *97*, 16−20.

(3) Liu, L.; Zhou, X.; Lu, Y.; Shi, H.; Ma, M.; Yu, T. Triple functional small-molecule-protein conjugate mediated optical biosensor for quantification of estrogenic activities in water samples. *Environ. Int.* **2019**, *132*, No. 105091.

(4) Qu, W.; Liu, Y.; Liu, D.; Wang, Z.; Jiang, X. Copper-mediated amplification allows readout of immunoassays by the naked eye. *Angew. Chem., Int. Ed.* **2011**, *50*, 3442−3445.

(5) Qu, Z.; Xu, H.; Xu, P.; Chen, K.; Mu, R.; Fu, J.; Gu, H. Ultrasensitive ELISA using enzyme-loaded nanospherical brushes as labels. *Anal. Chem.* **2014**, *86*, 9367−9371.

(6) Wei, Y.; Wang, D.; Zhang, Y.; Sui, J.; Xu, Z. Multicolor and photothermal dual-readout biosensor for visual detection of prostate specific antigen. *Biosens. Bioelectron.* **2019**, *140*, No. 111345.

(7) Ambrosi, A.; Airò, F.; Merkoçi, A. Enhanced gold nanoparticle based ELISA for a breast cancer biomarker. *Anal. Chem.* **2010**, *82*, 1151−1156.

(8) Liu, D.; Wang, Z.; Jin, A.; Huang, X.; Sun, X.; Wang, F.; Yan, Q.; Ge, S.; Xia, N.; Niu, G.; Liu, G.; Hight Walker, A. R.; Chen, X. Acetylcholinesterase-catalyzed hydrolysis allows ultrasensitive detection of pathogens with the naked eye. *Angew. Chem., Int. Ed.* **2013**, *52*, 14065−14069.

(9) Zhang, Q.; Zhao, B.; Yan, J.; Song, S.; Min, R.; Fan, C. Nanotube-based colorimetric probe for ultrasensitive detection of ataxia telangiectasia mutated protein. *Anal. Chem.* **2011**, *83*, 9191−9196.

(10) Ye, H.; Yang, K.; Tao, J.; Liu, Y.; Zhang, Q.; Habibi, S.; Nie, Z.; Xia, X. An enzyme-free signal amplification technique for ultrasensitive colorimetric assay of disease biomarkers. *ACS Nano* **2017**, *11*, 2052−2059.

(11) Gao, L.; Zhuang, J.; Nie, L.; Zhang, J.; Zhang, Y.; Gu, N.; Wang, T.; Feng, J.; Yang, D.; Perrett, S.; Yan, X. Intrinsic peroxidase-like activity of ferromagnetic nanoparticles. *Nat. Nanotechnol.* **2007**, *2*, 577−583.

(12) Asati, A.; Santra, S.; Kaittanis, C.; Nath, S.; Perez, J. M. Oxidase-like activity of polymer-coated cerium oxide nanoparticles. *Angew. Chem., Int. Ed.* **2009**, *48*, 2308−2312.

(13) Zhang, X. Q.; Gong, S. W.; Zhang, Y.; Yang, T.; Wang, C. Y.; Gu, N. Prussian blue modified iron oxide magnetic nanoparticles and their high peroxidase-like activity. *J. Mater. Chem.* **2010**, *20*, 5110−5116.

(14) Yang, N.; Huang, Y.; Ding, G.; Fan, A. In situ generation of prussian blue with potassium ferrocyanide to improve the sensitivity of chemiluminescence immunoassay using magnetic nanoparticles as label. *Anal. Chem.* **2019**, *91*, 4906−4912.

(15) Farka, Z.; Čunderlová, V.; Horáčková, V.; Pastucha, M.; Mikušová, Z.; Hlaváček, A.; Skládal, P. Prussian blue nanoparticles as a catalytic label in a sandwich nanozyme-linked immunosorbent assay. *Anal. Chem.* **2018**, *90*, 2348−2354.

(16) Fu, G.; Sanjay, S. T.; Dou, M.; Li, X. Nanoparticle-mediated photothermal effect enables a new method for quantitative biochemical analysis using a thermometer. *Nanoscale* **2016**, *8*, 5422−5427.

(17) Fu, G.; Sanjay, S. T.; Li, X. Cost-effective and sensitive colorimetric immunosensing using an iron oxide-to-Prussian blue nanoparticle conversion strategy. *Analyst* **2016**, *141*, 3883−3889.

(18) Lee, H. A.; Ma, Y.; Zhou, F.; Hong, S.; Lee, H. Material-independent surface chemistry beyond polydopamine coating. *Acc. Chem. Res.* **2019**, *52*, 704−713.

(19) Hong, S.; Kim, K. Y.; Wook, H. J.; Park, S. Y.; Lee, H.; et al. Attenuation of the in vivo toxicity of biomaterials by polydopamine surface modification. *Nanomedicine* **2011**, *6*, 793−801.

(20) Zhong, S.; Luo, R.; Wang, X.; Tang, L.; Wu, J.; Wang, J.; Huang, R.; Sun, H.; Huang, N. Effects of polydopamine functionalized titanium dioxide nanotubes on endothelial cell and smooth muscle cell. *Colloids Surf., B* **2014**, *116*, 553−560.

(21) Wu, C.; Fan, W.; Chang, J.; Xiao, Y. Mussel-inspired porous SiO_2 scaffolds with improved mineralization and cytocompatibility for drug delivery and bone tissue engineering. *J. Mater. Chem.* **2011**, *21*, 18300.

(22) Fan, B.; Fan, Q.; Cui, M.; Wu, T.; Wang, J.; Ma, H.; Wei, Q. Photoelectrochemical biosensor for sensitive detection of soluble CD44 based on the facile construction of a poly(ethylene glycol)/hyaluronic acid hybrid antifouling interface. *ACS Appl. Mater. Interfaces* **2019**, *11*, 24764−24770.

(23) Ju, K. Y.; Lee, Y.; Lee, S.; Park, S. B.; Lee, J. K. Bioinspired polymerization of dopamine to generate melanin-like nanoparticles having an excellent free-radical-scavenging property. *Biomacromolecules* **2011**, *12*, 625−632.

(24) Liu, Y.; Zhao, Y.; Fan, Q.; Khan, M. S.; Li, X.; Zhang, Y.; Ma, H.; Wei, Q. Aptamer based electrochemiluminescent thrombin assay using carbon dots anchored onto silver-decorated polydopamine nanospheres. *Microchim. Acta* **2018**, *185*, No. 85.

(25) Liu, Y.; Zhao, Y.; Zhu, Z.; Xing, Z.; Ma, H.; Wei, Q. Ultrasensitive immunosensor for prostate specific antigen using biomimetic polydopamine nanospheres as an electrochemiluminescence superquencher and antibody carriers. *Anal. Chim. Acta* **2017**, *963*, 17−23.

(26) Li, Y.; Xie, Y.; Wang, Z.; Zang, N.; Carniato, F.; Huang, Y.; Andolina, C. M.; Parent, L. R.; Ditri, T. B.; Walter, E. D.; Botta, M.; Rinehart, J. D.; Gianneschi, N. C. Structure and function of iron-loaded synthetic melanin. *ACS Nano* **2016**, *10*, 10186−10194.

(27) Ju, K. Y.; Lee, J. W.; Im, G. H.; Lee, S.; Pyo, J.; Park, S. B.; Lee, J. H.; Lee, J. K. Bio-inspired, melanin-like nanoparticles as a highly efficient contrast agent for T1-weighted magnetic resonance imaging. *Biomacromolecules* **2013**, *14*, 3491−3497.

(28) Lemaster, J. E.; Wang, Z.; Hariri, A.; Chen, F.; Hu, Z.; Huang, Y.; Barback, C. V.; Cochran, R.; Gianneschi, N. C.; Jokerst, J. V. Gadolinium doping enhances the photoacoustic signal of synthetic

melanin nanoparticles: A dual modality contrast agent for stem cell imaging. *Chem. Mater.* **2019**, *31*, 251−259.
(29) Chen, L.; Lin, Z.; Liu, L.; Zhang, X.; Shi, W.; Ge, D.; Sun, Y. Fe^{2+}/Fe^{3+} ions chelated with ultrasmall polydopamine nanoparticles induce ferroptosis for cancer therapy. *ACS Biomater. Sci. Eng.* **2019**, *5*, 4861−4869.
(30) Ejima, H.; Richardson, J. J.; Liang, K.; Best, J. P.; van Koeverden, M. P.; Such, G. K.; Cui, J.; Caruso, F. One-step assembly of coordination complexes for versatile film and particle engineering. *Science* **2013**, *341*, 154−157.
(31) Hong, S.; Wang, Y.; Park, S. Y.; Lee, H. Progressive fuzzy cation-π assembly of biological catecholamines. *Sci. Adv.* **2018**, *4*, No. eaat7457.
(32) Ju, K. Y.; Kang, J.; Chang, J. H.; Lee, J. K. Clue to understanding the janus behavior of eumelanin: Investigating the relationship between hierarchical assembly structure of eumelanin and its photophysical properties. *Biomacromolecules* **2016**, *17*, 2860−2872.
(33) Li, Y.; Xie, Y.; Wang, Z.; Zang, N.; Carniato, F.; Huang, Y.; Andolina, C. M.; Parent, L. R.; Ditri, T. B.; Walter, E. D.; et al. Structure and function of iron-loaded synthetic melanin. *ACS Nano* **2016**, *10*, 10186.
(34) Ortega, G. A.; Zuaznabar-Gardona, J. C.; Edilso, R. Electrochemical immunoassay for the detection of IgM antibodies using polydopamine particles loaded with PbS quantum dots as labels. *Biosens. Bioelectron.* **2018**, *116*, 30−36.
(35) Ngo, T. T. Immunoassay. *Curr. Opin. Biotechnol.* **1991**, *2*, 102−109.
(36) Porstmann, T.; Kiessig, S. T. Enzyme immunoassay techniques an overview. *J. Immunol. Methods* **1992**, *150*, 5−21.
(37) Negahdary, M.; Sattarahmady, N.; Heli, H. Advances in prostate specific antigen biosensors-impact of nanotechnology. *Clin. Chim. Acta* **2020**, *504*, 43−55.
(38) Sun, T.; Xia, N.; Yuan, F.; Liu, X.; Liu, L. A colorimetric method for determination of theprostate specific antigen based on enzyme-free cascaded signal amplification via peptide-copper(II) nanoparticles. *Microchim. Acta* **2020**, *187*, No. 116.
(39) Qian, Y.; Fan, T.; Wang, P.; Zhang, X.; Luo, J.; Zhou, F.; Yao, Y.; Liao, X.; Li, Y.; Gao, F. A novel label-free homogeneous electrochemical immunosensor based on proximity hybridization-triggered isothermal exponential amplification induced G-quadruplex formation. *Sens. Actuators, B* **2017**, *248*, 187−194.
(40) Gao, F.; Zhou, F.; Chen, S.; Yao, Y.; Wu, J.; Yin, D.; Geng, D.; Wang, P. Proximity hybridization triggered rolling-circle amplification for sensitive electrochemical homogeneous immunoassay. *Analyst* **2017**, *142*, 4308−4316.

https://dx.doi.org/10.1021/acsabm.0c01167
ACS Appl. Bio Mater. XXXX, XXX, XXX−XXX